Talanta 135 (2015) 7–17

Contents lists available at ScienceDirect

Talanta

journal homepage: www.elsevier.com/locate/talanta

Direct analysis of six antibiotics in wastewater samples using rapid high-performance liquid chromatography coupled with diode array detector: A chemometric study towards green analytical chemistry

Maryam Vosough [a,*], Masoumeh Rashvand [a], Hadi M. Esfahani [a], Kazem Kargosha [a], Amir Salemi [b]

[a] Chemistry and Chemical Engineering Research Center of Iran, P.O. Box 14335-186, Tehran, Iran
[b] Environmental Sciences Research Institute, Shahid Beheshti University, G.C., Tehran, Iran

ARTICLE INFO

Article history:
Received 14 October 2014
Received in revised form
19 December 2014
Accepted 22 December 2014
Available online 31 December 2014

Keywords:
Antibiotics
Direct analysis
HPLC–DAD
Second-order calibration
Wastewater

ABSTRACT

In this work, a rapid HPLC–DAD method has been developed for the analysis of six antibiotics (amoxicillin, metronidazole, sulfamethoxazole, ofloxacine, sulfadiazine and sulfamerazine) in the sewage treatment plant influent and effluent samples. Decreasing the chromatographic run time to less than 4 min as well as lowering the cost per analysis, were achieved through direct injection of the samples into the HPLC system followed by chemometric analysis. The problem of the complete separation of the analytes from each other and/or from the matrix ingredients was resolved as *a posteriori*. The performance of MCR/ALS and U-PLS/RBL, as second-order algorithms, was studied and comparable results were obtained from implication of these modeling methods. It was demonstrated that the proposed methods could be used promisingly as green analytical strategies for detection and quantification of the targeted pollutants in wastewater samples while avoiding the more complicated high cost instrumentations.

1. Introduction

Application of different second (or higher) order calibration methods for handling multi-dimensional chromatographic data is considered as an efficient strategy to extract qualitative and quantitative information from complex analytical data [1–3]. In this regard, samples from sewage treatment plants (STPs) are amongst the most relevant examples which their analysis might produce such data. Highly contaminated background and the corresponding unwanted signals and coeluting matrix constituents, might be too difficult to be handled using the conventional methods of chromatographic analysis. Sample preparation procedures, sometimes, help to partially overcome such problems via selective extraction and cleanup steps but they inherently add to the complexity of the environmental analytical approach. However, hyphenated chromatographic systems have provided the possibility of using high-order calibration methods in various fields, such as environmental analysis [4–8], bioanalysis [9–12] and food analysis [13–16], for dealing with unknown interferences and separating their two-way analytical signals from target analytes in a mathematical way by exploiting second-order advantage [17].

There are different multivariate algorithms that benefit from the second-order advantage and can be adapted to the three-way data obtained from hyphenated chromatography. Generalized rank annihilation method (GRAM) [18], direct trilinear decomposition (DTLD) [19], parallel factor analysis (PARAFAC) [20], PARAFAC2 [21], alternating trilinear decomposition (ATLD) [22], self-weighted alternating trilinear decomposition (SWATLD) [23], alternating penalty trilinear decomposition (APTLD) [24], multivariate curve resolution alternating least squares (MCR–ALS) [25,26], bilinear least squares (BLLS) [27],and also unfolded partial least squares (U-PLS) [28] as well as multi-way PLS (N-PLS) [29], both combined with residual bilinearization (RBL) [30–32], are among these algorithms. In a newly published tutorial, multi-way calibration methods based on second- and higher-order data generation have been discussed with emphasis on the most popular multi-way data [33].

Since the retention time shifts and peak shape changes usually occur between different chromatographic runs, a proper alignment algorithm is required prior to application of the trilinear algorithms [34–37].Among the second-order algorithms, PARAFAC2 and MCR/ALS tolerate some degree of deviations from trilinearity in three-dimensional data. MCR/ALS has been shown to be an excellent tool

* Corresponding author. Tel.: +98 21 44580720; fax: +98 21 44580762.
E-mail address: vosough@ccerci.ac.ir (M. Vosough).

http://dx.doi.org/10.1016/j.talanta.2014.12.036
0039-9140/

for modeling the LC–DAD data in the presence of retention time shifts in a set of chromatograms [4–9,38]. Also, there are some reports on chromatographic data analysis using PARAFAC2, a variant of PARAFAC, implementing its tolerability to the flexibility of the profiles (in one dimension) from sample to sample [14,38,39]. On the other hand, second-order multivariate calibration based on latent structure modeling methods, such as U-PLS/RBL and N-PLS/RBL, are in principle able to cope with trilinearity deviation in data sets. However, the success of these modeling methods depends on availability of a sufficiently large and representative set of calibration samples [40]. To the best of our knowledge there are very few publications on the application of RBL-based methods for hyphenated chromatographic systems; the work of Gil García et al., as the first application of U-PLS/RBL on HPLC–DAD data for determination of eight tetracycline antibiotics in effluent wastewater samples [41], the use of N-PLS/RBL on the data from HPLC with fast-scanning fluorescence detection (FSFD) for the determination of fluoroquinolones (FQs) [40] and the use of U-PLS/RBL for the determination of dyes in beverage by the LC–DAD method [42]. However, considering the significant differences in samples and also in the complexity of the problem, various situations were faced in each of the mentioned reports. In the first work, no chromatographic alignment was applied, in the second, the chromatographic data was aligned and in the last work the chromatograms were too difficult to be aligned because of the severe coelution problem. Also, recently, a fast HPLC procedure has been proposed for quantitative determination of fluoroquinolones in water samples by means of four- and three-way modeling of excitation-emission fluorescence matrices at different elution times [43]. The performance of three algorithms; U-PLS/residual trilinearization (RTL, as a natural extension to RBL), PARAFAC, and MCR/ALS have been compared with each other. The predictive ability and figures of merits have been also compared between second-order and third-order data.

The main goal in the presented study is quantification of six antibiotics in STP influent and effluent, through a simple method of direct injection into the HPLC–DAD system. This approach is oriented towards a green analytical methodology by reducing the amounts of used-wasted materials, such as solvents, sorbents and so on. Amoxicillin (AMX), metronidazole (MET), sulfadiazine (SDZ), sulfamerazine (SMR), ofloxacine (OFX) and sulfamethoxazole (SMX), were selected as the target analytes, from various classes of antibiotics. In fact, occurrence of these emerging contaminants in wastewaters and natural water resources has been frequently studied [44–46]. These pharmaceuticals and their metabolites and degradation products, can impact the aquatic environment via various transport paths. Consequently, as a result of their long time occurrence in the environment, antimicrobial-resistant bacteria can appear [47]. In the vast majority of the studies on the determination or monitoring of antibiotics, solid phase extraction (SPE) on various sorbents has been utilized for extraction/pre-concentration purposes, followed by HPLC with UV, DAD, mass spectrometry (MS) or tandem mass spectrometry (MS/MS) detection systems [44–46,48].The authors recently proposed a SPE–LC–DAD for simultaneous determination of five antibiotics in effluent wastewater samples, in approximately 4 min with the aid of chemometrics tools [5]. In that work, a successful application of MCR/ALS modeling without any preprocessing step, through standard addition strategy, was reported. Decreasing the number of sample preparation steps, lead to significant simplification of the optimization procedure and also to reducing the time and cost of the entire analysis. Among the studies for direct analysis of selected antibiotics, the works by Teixeira et al. [49] and Yu et al. [50] can be pointed. In the former, a direct screening of five antibiotics in 35 min using HPLC–DAD was proposed and in the latter, UPLC/MS/MS was used for simultaneous determination of 11 pharmaceutical and personal care products (PPCPs) in influent and effluent wastewater samples, without SPE step. During the last decade, MS/MS has become a powerful analytical technique which offers adequate selectivity and sensitivity for the analysis of complex matrices, as well as the screening purposes and studying the structure of unknown metabolites, etc. However, in addition to the cost of the instrumentation, possibility of matrix effect (signal suppression or signal enhancement) is a main drawback for using this system in complex samples. This may justify the efforts to propose rapid, simple, cost-effective and reliable complementary methodologies for multi-target determination in wastewater samples, based on the less sophisticated detection systems such as DAD.

In brief, we proposed the presented novel strategy for direct determination of six antibiotics in wastewater samples with different complexities, in less than 4 min using a fast gradient elution program. Because of inevitable coelution problems between analytes and matrix constituents, second-order modeling methods were exploited. Applicability of U-PLS/RBL for modeling of these analytes in the presence of different interferences was investigated and the results were compared with the well-known MCR–ALS method on raw HPLC–DAD data.

2. Experimental and methods

2.1. Reagents and materials

Analytical standards of AMX, MET, SDZ, SMR, OFX and SMX were purchased from Sigma-Aldrich (USA), all of high purity, 99.8%. Stock standard solutions (0.8–1.2 mg mL^{-1}) were prepared, every four weeks, in methanol (MET, SDZ, SMR and SMX) or water (AMX and OFX) and stored in amber vials in a freezer (−18 °C).Working standard solutions were prepared by successive dilution of the stock solutions with methanol/milli-Q water mixture (1:1, v/v) just before use and kept at 4 °C in amber vials. HPLC grade methanol was from Merck (Germany). Hydrochloric acid (32%) and orthophosphoric acid (85%), potassium di-hydrogen phosphate and sodium hydroxide were of analytical reagent quality, from Merck. HPLC grade water for chromatographic separation was prepared using a Milli-Q water purification system from Millipore (USA) equipped with a 0.22 μm filter. Solvents as well as calibration and real samples were filtered through 0.22 μm nylon membrane filter (Varian, USA) before HPLC analysis.

2.2. HPLC apparatus and procedure

Chromatographic analyses were performed using an Agilent 1200 HPLC system (Agilent Technologies Inc., USA) consisting of a quaternary pump, Rheodyne 7725 manual injector and a 200 μL injection loop, a degasser system, a column oven compartment and a Hewlett-Packard 1200 series photo diode-array detector. Chromatographic separation was carried out on an end-capped RP-18 column (70 mm × 4.6 mm and 5 μm of particle size) with a RP-18 (4 mm × 4.6 mm) guard column. The mobile phase constituents, (A) phosphate buffer (50 mM, pH = 3) and (B) methanol, were used in a gradient elution program as follows; 75% A as the starting mobile phase composition, descended to 35% in 4 min. The mobile phase then returned to the initial composition in 1 min and the analytical column was allowed to get to the equilibrium before the next run. Mobile phase flow rate was 1.0 mL min^{-1} and the column oven temperature was set at 25 °C. The data were collected using Chemstation software package (version B.03.01) for LC.

2.3. Sample collection and preparation

Wastewater influent and effluent samples were collected from a sewage treatment plant in Tehran (Iran), and transferred to the

laboratory in pre-cleaned amber glass bottles. Upon entry, the samples were centrifuged at 4000 rpm for 10 min (Centrifuge 320R, Hettich, Germany)and then filtered through a 0.22 μm membrane filter, stored in darkness at 4 °C and were processed within 72 h.

2.4. Calibration and validation samples

A set of 15calibration samples (C1–C15), containing 1–200 μg $L^{-1}$of SDZ, 5–200 μg $L^{-1}$of MET, 1–100 μg $L^{-1}$of SMR, 10–200 μg $L^{-1}$of SMX and 5–200 μg L^{-1}ofboth AMX and OFL, were prepared in 10.00 mL volumetric flasks. The chromatogram of the mixed standards showed five distinct regions consisting of one overlapping part where SDZ and MET co-eluted and four distinct regions where the remaining four analytes had been completely resolved. So, the concentrations of SDZ and MET in the calibration set were designed in a random manner and the other four analytes in an increasing way and all were analyzed in triplicate.

The set of validation samples consisted of six STP effluent (SE-1 to SE-6) and five STP influent (SI-1 to SI-5) samples which were spiked at different concentration levels and used for recovery studies (see Table 1).The spiked samples were shaken vigorously, then filtered through 0.22 μm Nylon syringe filter and directly injected into the HPLC–DAD system. The samples SE-6 and SI-5 were also prepared and analyzed in triplicate to evaluate the repeatability of the method.

2.5. Data analysis

2.5.1. MCR–ALS

MCR/ALS provides a useful tool which can be used for decomposing a chromatographic landscape containing overlapping signals into the contributing elution profile and the spectral profiles of individual components [25,26]. The use of this method for the analysis of a chromatographic 3-way array requires an augmentation step. For this purpose, a global data matrix is created along the mode which is suspected to break the trilinearity. Since the source of deviation from trilinear structure is the retention time shift and/or variation of profile shapes between different runs, a column-wise augmented matrix is usually made in hyphenated chromatographic systems, such as HPLC–DAD. The bilinear decomposition for an augmented data matrix **D**, contains *K* calibration matrices and one test sample and is expressed as:

$$\mathbf{D} = \mathbf{C}\mathbf{S}^T + \mathbf{E} \quad (1)$$

where the rows in matrix **D** (*I* (number of elution times in each sample) × (*K* (number of calibration samples)+*1*), *J* (number of wavelengths)) contain the recorded spectra as a function of time, the columns of **C** (*I* × (*K*+1), *N*) contain the elution time profiles of the compounds (*N*) involved in the process for all sub-matrices, the columns of **S** (*N, J*) represent their corresponding spectra, and **E** (*I* × (*K*+1), *J*) is a matrix of residuals not fitted by the model. In MCR–ALS, decomposition of **D** is achieved by iterative least-squares minimization of ||**E**||, under suitable constraining conditions, i.e. correspondence criterion, non-negativity in the spectral profiles, and unimodality and non-negativity in the time profiles. MCR–ALS is initialized by an initial estimation of the spectra or concentration profiles for each of the involved compounds. In this work, the purest spectra based on SIMPLISMA (simple interactive self-modeling mixture analysis) were considered as initial estimates of involved components [51].

After decomposition of **D** by MCR–ALS, the analyte concentration scores, which are defined as the area under each of the resolved chromatographic profiles in $\mathbf{C}_{aug}$, were computed. Then, these values were employed to build a pseudo-univariate calibration graph versus the analyte concentration, which in turn was used in predicting the analyte concentration in the test samples through interpolation of the test sample score.

2.5.2. U-PLS/RBL

Briefly, in the first step of U-PLS/RBL algorithm, a conventional U-PLS model was constructed. This step resulted a set of loadings **P** and weight loadings **W** (both of the size JK × A, where A was the number of the latent factors selected by leave-one-out cross-validation [28]), as well as regression coefficients **v** (size A × 1). While there are no unexpected interferences in the test sample, **v** can be employed to estimate the concentration of the analyte:

$$y_u = \mathbf{t}_\mathbf{u}^T\mathbf{v} \quad (2)$$

where $\mathbf{t}_u$ is the test sample score, obtained by projection of the unfolded data of the test sample $\mathbf{X}_u$ onto the space of A latent factors:

$$\mathbf{t}_u = (\mathbf{W}^T\mathbf{P})^{-1}\mathbf{W}^T\mathrm{vec}(\mathbf{X}_u) \quad (3)$$

If unexpected components exist in $\mathbf{X}_u$, an additional step can be added to U-PLS procedure, which is called residual bilinearization [30–32].In this situation, the sample signal can be decomposed into two parts; one which can be modeled using calibration latent variables, one which cannot be modeled by these variables. RBL is based on singular value decomposition (SVD) modeling of the interfering components that are present in the un-modeled part of the signal. So, the unexpected profiles can be estimated by minimizing the norm of the residual vector $\mathbf{e}_u$, computed while fitting the sample data to the sum of the relevant contributions. When there is just one unexpected component, then:

$$\mathrm{vec}(\mathbf{X}_u) = \mathbf{P}\mathbf{t}_u + \mathrm{vec}\left[g_{unx}\mathbf{b}_{unx}(\mathbf{c}_{unx})^T\right] + \mathbf{e}_u \quad (4)$$

in which $\mathbf{b}_{unx}$ and $\mathbf{c}_{unx}$ are the left and right eigenvectors of $\mathbf{E}_p$ and g_{unx} is a scaling factor. During RBL procedure, **P** is kept constant at the calibration values and $\mathbf{t}_u$ is varied until $\|\mathbf{e}_u\|$ is minimized. So, the interferent profiles can be estimated by SVD of $\mathbf{E}_p$ as follows:

$$(g_{unx}, \mathbf{b}_{unx}, \mathbf{c}_{unx}) = \mathrm{SVD}_1(\mathbf{E}_p) \quad (5)$$

Where **E**p is the $J \times K$ matrix obtained after reshaping the $JK \times 1$PLSresidual vector, and SVD_1 indicates taking the first principal component. By minimization of $\|\mathbf{e}_u\|$in Eq. (4) the analyte concentrations can be obtained by Eq. (2), by introducing the final $\mathbf{t}_u$ vector found in the RBL procedure. The number of interferents can be assessed by comparing the final residuals with the level of the instrumental noise. It is necessary to note that when there is more than one interfering component in a data matrix, their corresponding profiles, provided by SVD analysis of $\mathbf{E}_p$, no longer

Table 1
Composition of the validation samples obtained by spiking different antibiotics concentrations on influent and effluent wastewaters.

Sample	Component (μg L^{-1}) AMOX	SDZ	MET	SMR	OFL	SMX
Influent						
SI-1	48.1	12.2	6.5	8.6	7.3	7.3
SI-2	10.2	4.7	7.0	2.1	10.1	4.8
SI-3	30.6	32.5	44	43.6	30.5	17.2
SI-4	40.6	14.8	8.3	4.4	24.2	14.6
SI-5	18.2	45.2	14.3	36.2	41.1	40.8
Effluent						
SE-1	8.2	12.2	6.5	8.6	7.3	5.8
SE-2	10.2	7.3	8.3	10.3	5.6	9.8
SE-3	16.4	8.1	13.2	3.5	8.5	17.2
SE-4	40.6	14.8	8.3	4.4	24.2	14.6
SE-5	43.6	32.5	31.3	48.1	8.9	17.2
SE-6	30.6	26.2	18.4	18.3	46.3	30.1

resemble the true interferent profiles, due to the orthonormality restriction. The full description of the method can be found elsewhere [32].

2.6. Software

HPLC–DAD data, gathered by Chemstation software, exported as Microsoft Excel® file for further processing. Routines for MCR–ALS were available at (http://www.ub.edu/mcr/welcome.htm) and all algorithms were written in MATLAB (version 7.2.0.232 R2006a, The Mathworks, Natick, MA). U-PLS/RBL was performed using the MVC2 routine, an integrated MATLAB toolbox for second-order calibration developed by Olivieri et al. [52].

3. Results and discussion

3.1. Characterization of the instrumental method

The instrumental method was validated, primarily, through injection of pure analytes at different concentration levels. Signal detection, for univariate quantitative purposes, was carried out at 230 nm for AMOX, 270 nm for SDZ, SMR and SMX, 318 nm for MET and 294 for OFL. Then, the conventional calibration curves were constructed using the results of triplicate analysis of a set of seven concentration levels for each analyte in the range of 1–200 ppb ($r^2 > 0.993$). The corresponding analytical figures of merit, under the optimum HPLC conditions (Section 2.2.), are sown in Table 2. The lack-of-fit test was used (Statgraphics Centurion XVI, V 16.1.11) to confirm the linearity of the assay in each calibration range. The lack-of-fits in the ANOVA tables showed the p-values greater than 0.05, so the adequacy of the linear models was proved for all six calibration curves at 95% confidence level. The repeatability was tested for an intermediate concentration point ($n=4$) and RSD values less than or equal to 6.88% were obtained. Limits of detection (LODs) were calculated using signal-to-noise ratio ($S/N=3$) divided by the slope of the calibration curve. Limits of quantification (LOQs) were experimentally estimated from injection of calibration samples, serially diluted until the relative standard deviation (RSD) of the signal was equal to 10% [53].

3.2. Second-order modeling using MCR–ALS and U-PLS/RBL

As stated before, the main aim of the present study was to develop a short run time direct injection HPLC method as a green strategy, in conjunction with second-order algorithms, preferably without signal-preprocessing steps and without losing data accuracy and precision. So at the beginning, a chromatographic methodology with a fast elution pattern was developed. Using a short column and optimizing the composition of the mobile phase were considered as the most effective variables in this regard (see Section 2.2.). Fig. 1 shows the chromatographic landscape obtained for six analytes with the concentration values between 10–50 μg L^{-1}. As can be seen, SMX was the last eluted analyte (3.6 min) and except SDZ and MET, complete separation of the analytes was achieved in a very short time. So, it was expected that because of the immense variety of the matrix contaminants in wastewater samples, the proposed HPLC method would almost certainly produce some coelution problems, making the accurate analysis almost impossible through univariate calibration strategy. Although, as shown in the literature [49], even by proposing long chromatographic run times in similar situations, there was no guarantee for physical removal of the interferences.

Table 2
Analytical figures of merit for the determination of the six antibiotics by univarite calibration.

Analyte	Linear range (μg L^{-1})	R^2	RSD %[a]	LODs (μg L^{-1})	LOQs (μg L^{-1})
AMOX	5–200	0.997	5.87	1.3	5.0
SDZ	5–200	0.999	6.19	1.4	5.0
MET	5–200	0.993	6.88	0.40	5.0
SMR	1–100	0.999	6.59	0.05	1.0
OFL	5–200	0.999	6.77	1.1	5.0
SMX	10–200	0.999	2.59	2.1	10.0

[a] Relative standard deviation for six replicates analysis of 50 μg L^{-1} of each analyte.

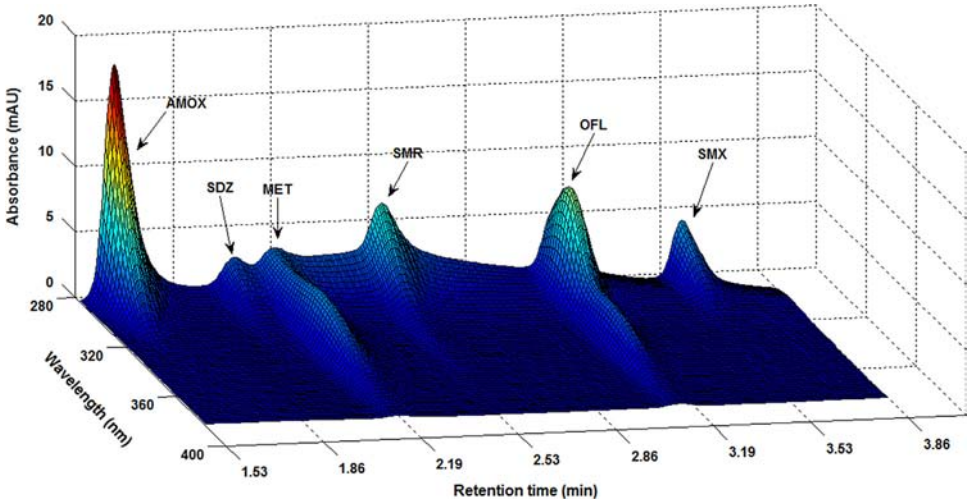

Fig. 1. Three dimensional representation of the LC–DAD chromatograms of a standard mixture of antibiotics at concentration of 10 μg L^{-1} of AMOX, 20 μg L^{-1} of SDZ and 50 μg L^{-1} of MET, SMR, OFL and SMX. The analytes of interest are indicated.

DAD signal was recorded between 220 and 400 nm with the spectral resolution of 2 nm and integration period of 0.4 s per spectrum. Thus, every chromatographic record was a matrix of 900×90 for elution time region of 1.4–4.0 min and the detection wavelength range. Then, the exported data for each sample was partitioned into five or six regions (depending on samples) in order to simplify the analysis or in some cases, to make the data analysis possible (see below). Table 3 shows the employed elution time and spectral regions for analysis of the samples using second-order modeling methods. In Fig. 2, the chromatograms of the spiked influent and effluent (inserted figure) wastewater samples in multiple wavelengths have been shown. The complexity of the chromatograms and appearance of unexpected components in the retention time region of the analytes can be clearly observed and are, as expected, more serious in the influent samples. In fact, comparing the chromatographic patterns of the influent and effluent samples in this figure showed that wastewater treatment process had significantly removed or reduced interfering organics from the raw sewage. Considering different coelution problems encountered in this work, second-order data analysis was performed separately on each region of the data matrices of the validation samples (Table 1, Section 2.4.).

3.2.1. *Effluent samples*

The chromatographic data matrices obtained through analysis of effluent samples were divided into five regions (see Table 3). So, except the region 2, which was considered for the simultaneous modeling of SDZ and MET, the rest of the analytes were modeled separately in their matrix subsets. Matrix interferences were expected to be present in each subset with different degrees of coelution and spectral similarities. Resolution and quantification of the effluent samples using MCR/ALS were attempted first. For this purpose, individual models were built by column-wise augmentation of 15 calibration sub-matrices with each of the unknown samples (global matrix **D**). Selecting matrix augmentation in the time direction was because of the fact that there was a retention time shift between unknown samples and calibration samples. The number of components in the matrix **D** was determined by SVD.

Table 3
The selected chromatographic and spectral regions for MCR–ALS and U-PLS/RBL modeling of effluent and influent samples and the number of factors which is necessary to model each region.

Analyte/ peak number	Scan no. (Retention time, min)	Scan no. region (Time region, min)	Spectral index no. (Wavelength region, nm)	MCR/ ALS factors[a]	U-PLS/RBL (unexpected Components[b])
AMOX (1)	255 (1.69)	240–260 (1.60–1.73)	20–106 (228–400)	3/2	3/3
SDZ(2)	304 (2.02)	293–313 (1.95–2.08)	31–106 (250–350)	2/–	1/–
MET(3)	325 (2.16)	311–342 (2.07–2.27)	56–106 (300–400)	4/–	1/–
SMR(4)	393 (2.61)	370–410 (2.46–2.73)	31–106 (250–400)	3/2	3/1
OFL(5)	476 (3.16)	460–500 (3.06–3.32)	31–106 (250–400)	2/2	3/2
SMX(6)	542 (3.60)	530–570 (3.53–3.69)	50–106 (288–348)	3/2	1/1
SDZ, MET[c]	304,325	290–355 (1.93–2.35)	41–106 (250–400)	–/4	–/1

[a] Number of MCR–ALS factors in influent/effluent samples. For effluent samples, SDZ and MET have been modeled in a common region (last row).
[b] Number of U-PLS/RBL unexpected components in influent and effluent samples. For effluent samples, SDZ and MET have been modeled in a common region (last row).
[c] The region which is selected for modeling of SDZ and MET together in effluent samples.

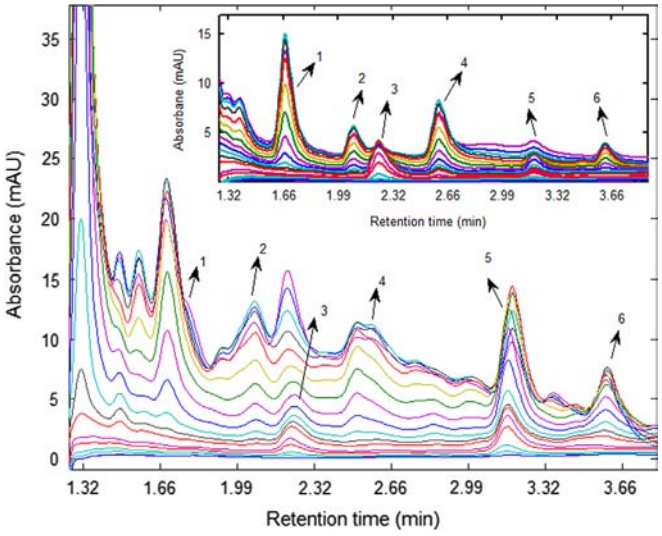

Fig. 2. Chromatographic profile of a typical spiked influent wastewater sample with 30 μg L^{-1} of AMOX, 46 μg $L^{-1}$of SDZ, 28 μg $L^{-1}$of MET, 26 μg L^{-1} of SMR, 18 μg L^{-1} of OFL and SMX, monitored at multiple wavelengths (every 3rd wavelength has been shown for more clarity). The insert plot shows the effluent sample of the same WWTP spiked with 17 μg $L^{-1}$of AMOX, 9 μg $L^{-1}$of SDZ, 48 μg $L^{-1}$of MET, 32 μg L^{-1} of SMR, 44 μg $L^{-1}$of OFL and 43 μg $L^{-1}$of SMX. (1) AMOX, (2) SDZ, (3) MET, (4) SMR, (5) OFL, and (6) SMX.

Then, using this number and proper initial estimate, MCR/ALS modeling of matrix D (without further pre-processing step) was started. The number of components was then updated for each sample according to the appropriate solution parameters, such as least squares fitting values, qualitative and quantitative results. The ALS parameters such as the convergence criterion and the constraints mentioned in Section 2.5.1. Finally, highly acceptable fitting values were obtained through applying MCR/ALS for all regions of effluent samples.

An example of the resolved elution and spectral profiles in the presence of the matrix interferences is shown in Fig. 3 for the MCR/ALS analysis of region 2 (sample SE-5 in Table 1). A three dimensional representation of the mentioned subset which clearly shows the complexity of this region is depicted in Fig. 3(A). In the subplot (B), four components containing SDZ and MET and two interferences can be observed. The elution profiles of the analytes were resolved successfully in the presence of unknown interfering peaks. The spectral profiles resolved by the algorithm are also shown in Fig. 3(C). This figure clearly confirms the resolution quality, and also high spectral matching between the predicted profiles and the normalized pure ones. The process was successfully repeated for the other sub-matrices and all spiked samples with various number of components. This number varied between 2 (for SMR) and 4 (for SDZ and MET) (Table 3).The concentration prediction results corresponding to the application of MCR/ALS to the set of six unknown samples (containing an un-spiked sample) have been shown in Table 4. As can be seen, the recovery values were acceptable for most of the samples. Also, standard deviation values (SD), root-mean square error of prediction values (RMSEP) and relative error of prediction (REP) have been calculated and were acceptable for most of the analytes, considering the complexity of the samples, the amounts of spiked values and using no preprocessing steps. Notably, the worst quantitative results were achieved for MET, possibly due to the large overlapping between this analyte and the interfering compounds and relatively low spiked concentration.

On the other hand, U-PLS/RBL was considered as a second-order modeling method to analyze each sub-matrix individually, using a vectorized calibration matrix, **X.** During U-PLS/RBL on each

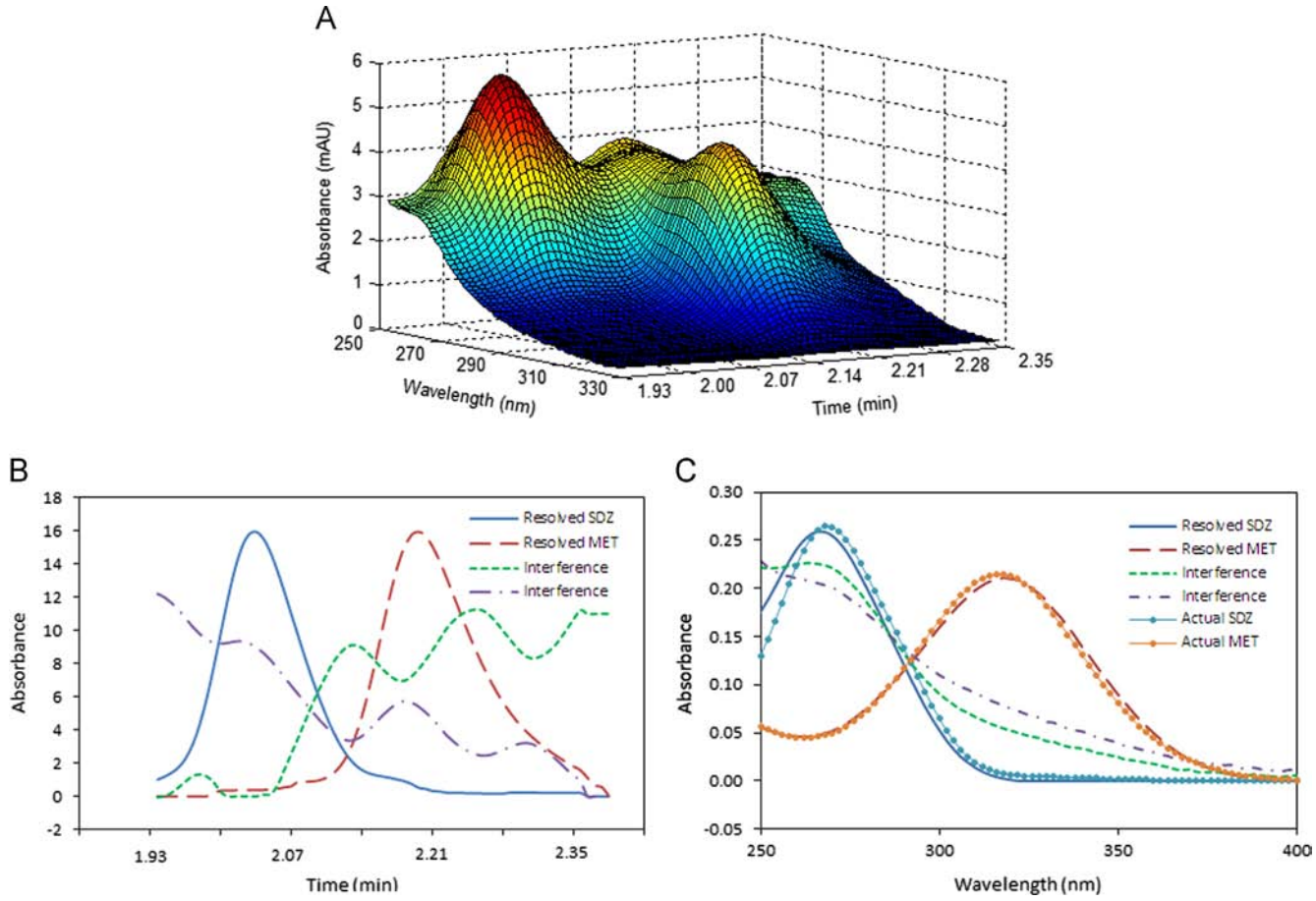

Fig. 3. Three dimensional representation of the second effluent sample region (1.93–2.35 min, Table 3), corresponding to SDZ and MET(spiked sample SE-5, Table 1) (A).Time profiles extracted by the MCR/ALS algorithm for analyzing this region, containing SDZ (*blue solid line*) and MET (*red long dash line*), two interfering compounds (*violet dot line and green short dash line*) (B).Corresponding spectral profiles recovered by MCR–ALS modeling for this region together with the normalized actual spectral profiles for SDZ (*blue solid line with circle marker*) and MET (*red solid line with circle marker*) (C) (For interpretation of the references to color in this figure legend, the reader is referred to the web version of this article.)

region of the chromatograms, the number of calibration latent variables for each analyte was set to one (confirmed with leave-one-out cross validation procedure), while different numbers of unexpected components (N_{unx}) were utilized in the RBL procedure. This was carried out by analyzing the prediction residuals for the unknown samples, $\mathbf{s_u}$, as a function of a trial number of unexpected components. When $\mathbf{s_u}$ was stabilized at a value comparable with the instrumental noise (ca. 0.07 absorbance units for this system), the correct number of unexpected components could be determined. Another considerable point in the U-PLS/RBL analysis was the higher quality of the results in case of trilinearity correction. Although U-PLS/RBL, as a latent based structure modeling, did not require a data set with perfect trilinear structure, we obtained more satisfactory results by performing retention time alignment [34]. Fig. 4 shows the deconvoluted elution and spectral profile related to the unexpected component present in the region 2 of sample SE-5.The number of the unexpected components in this region was set to one. This number which depended on the number of matrix interferences, the background contribution and the success of shift alignment method, was further confirmed by the quantitative results. In fact, the resolved unexpected component in this plot somehow resembled to the matrix interferences profiles which had been resolved using MCR/ALS method. However, different assumptions of the two methods applied through deconvolution process and implementation of unimodality restriction, could be a reason for providing different number of interfering components between two algorithms. In Table 4, the results of concentration prediction corresponding to application of U-PLS/RBL to a set of six spiked and one non-spiked effluent samples have been shown. As can be seen, in spite of the matrix complexity, acceptable and comparable results were obtained by MCR/ALS, for most of the samples. Table 4 also shows the SD, RMSEP and REP % values for U-PLS/RBL modeling of six analytes. The best results were obtained through analysis of regions 1 and 4 for determination of AMOX and OFL, respectively. The most interesting difference between predictive ability of the two methods can be seen by comparing REP% values for MET by MCR/ALS (34.2) and U-PLS/RBL (15.2), which showed a significant enhancement in prediction ability. Considering the recovery values between 70 and 120%, the number of predictions out of this range is higher for MCR/ALS than U-PLS/RBL. Compared with the calculated parameters of MCR/ALS predictions, it could be stated that the results of U-PLS/RBL were better for SDZ, MET and SMX, comparable for AMOX and OFL and was worse for SMR. Standard deviations were comparable for SDZ, SMR and OFL but were lower by U-PLS/RBL for AMOX, MET and slightly better by MCR/ALS for SMX. So, it can be stated that almost comparable results in accuracy and precision have been obtained from two mentioned methods for effluent samples.

The analytical figures of merit for the multivariate analysis of the effluent sample were calculated by modeling the data sets through U-PLS/RBL and MCR/ALS, based on the recently derived sensitivity equations [54,55]. The limits of detection were calculated as 3.3 times the standard deviation ($n=3$) of the predicted concentration for the blank effluent sample (or containing a low

Table 4
MCR–ALS and U-PLS/RBL predicted concentrations on the validation samples obtained by spiking different antibiotics amount on a real effluent wastewater sample.

sample	Component ($\mu g\ L^{-1}$)[a]					
	AMOX	SDZ	MET	SMR	OFL	SMX
MCR–ALS						
Unspiked	−0.5	0.4	−0.2	−0.6	5.2	0.2
SE-1	8.2 (100.0)	14.1(115.5)	4.9 (75.4)	4.4 (51.2)	6.3 (86.3)	5.9 (101.7)
SE-2	10.8 (105.8)	6.9 (94.5)	9.1 (109.6)	9.8 (95.1)	5.1 (91.1)	12.2 (124.5)
SE-3	20.9 (127.4)	12.2 (150.6)	5.6 (42.2)	3.3 (94.3)	9.2 (108.2)	12.8 (74.7)
SE-4	28.5 (70.2)	16.0 (108.1)	9.7 (116.8)	2.8 (63.6)	25 (103.3)	9.2 (63.0)
SE-5	36.1 (82.7)	25.6 (79.1)	21.0 (67.1)	50.7 (105.4)	8.1 (91.1)	12.8 (74.4)
SE-6	37.4 (122.2)	23.5 (89.7)	13.1 (71.2)	13.8 (75.4)	44.6 (96.3)	24.4 (81.1)
SD[b]	5.6	2.2	1.1	0.52	1.3	0.77
RMSEP($\mu g\ L^{-1}$)[c]	6.7	3.5	5.7	2.8	1.0	4.2
REP (%)[d]	23.3	18.4	34.2	12.9	4.5	23.9
U-PLS/RBL						
Unspiked	0.07	−0.3	−0.6	0.2	1.6	0.3
SE-1	8.6 (104.8)	10.8 (88.7)	7.7 (118.4)	8.9 (103.5)	6.2 (84.9)	5.9 (101.7)
SE-2	8.7 (85.2)	4.9 (67.1)	8.0 (96.4)	6.9 (67.0)	3.9 (70.0)	9.5 (96.9)
SE-3	19.5 (119.1)	8.5 (104.8)	14.3 (108.1)	2.1 (60.6)	6.2 (73.2)	16.5 (96.0)
SE-4	31.0 (76.4)	13.9 (93.8)	9.5 (114.8)	4.0 (91.0)	23.2 (96.1)	12.6 (86.6)
SE-5	32.6 (74.8)	27.2 (83.7)	36.2 (115.6)	56.2 (116.8)	7.6 (85.4)	16.5 (95.9)
SE-6	29.4 (96.1)	25.8 (98.5)	21.7 (118.0)	17.0 (92.9)	44.8 (96.7)	28.3 (93.9)
SD	2.2	2.2	0.60	0.50	1.3	1.9
RMSEP($\mu g\ L^{-1}$)	6.1	2.5	2.5	3.7	1.5	1.2
REP (%)	21.4	12.9	15.2	16.9	6.8	6.7

[a] Values between parentheses correspond to recovery % of spiked amount.
[b] Standard deviation values for three replicates analysis of sample SE-6.
[c] Root mean square error of prediction, RMSEP $\left(\mu g\ L^{-1}\right) = \left[\frac{1}{n}\sum_{n=1}^{n}(c_{add.} - c_{pred.})^2\right]^{1/2}$ where n is the number of unknown samples, $c_{add.}$ and $c_{pred.}$ are the added and predicted concentrations, respectively.
[d] Relative error of prediction, $\mathrm{REP} = 100 \times \left(\frac{\sum_{n=1}^{n}(c_{add.} - c_{pred.})^2}{\sum_{n=1}^{n} c_{add.}^2}\right)^{1/2}$.

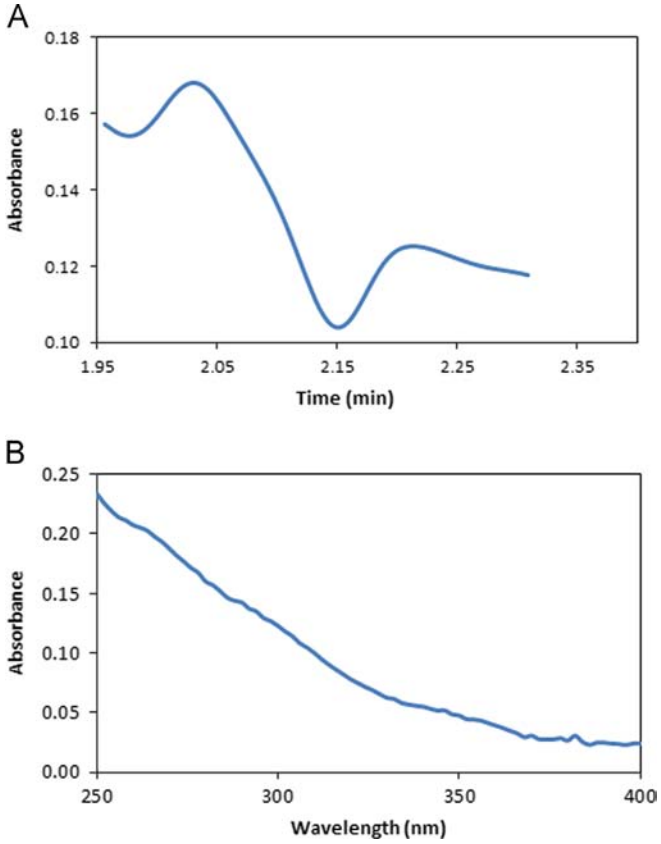

Fig. 4. Estimated elution time (A) and spectral profiles (B) for the unexpected component of the second effluent sample region (spiked sample SE-5, Table 1) by U-PLS/RBL.

Table 5
Multivariate figures of merit for determination of selected antibiotics in effluent samples by MCR–ALS and U-PLS/RBL modeling.

		AMOX	SDZ	MET	SMR	OFL	SMX
MCR–ALS	Sensitivity[a]	0.4	0.07	0.2	1.2	1.1	0.4
	[(Analytical sensitivity)$^{-1}$][b]	0.2	0.9	0.3	0.05	0.06	0.2
	LOD ($\mu g\ L^{-1}$)[c]	0.6	3.1	0.9	0.2	0.2	0.6
	LOQ ($\mu\ gL^{-1}$)[d]	1.7	9.5	2.8	0.5	0.6	1.8
U-PLS/RBL	Sensitivity[e]	1.5	0.4	0.6	0.2	0.4	0.1
	[(Analytical sensitivity)$^{-1}$][b]	0.1	0.2	0.1	0.3	0.2	0.7
	LOD ($\mu g\ L^{-1}$)[f]	0.1	0.6	0.4	1.1	0.6	2.3
	LOQ ($\mu g\ L^{-1}$)[d]	0.4	1.7	1.2	3.5	1.7	7.0

[a] Sensitivity was calculated according to Ref. [54].
[b] Analytical sensitivity was calculated as the ratio between sensitivity and instrumental noise.
[c] LOD: limit of detection was calculated according to Ref. [54].
[d] LOQ: limit of quantification was calculated as LOD × (10/3.3).
[e] Sensitivity was calculated according to Ref. [55].
[f] LOD: limit of detection was calculated according to Ref. [55].

analyte concentration) divided by the sensitivity (SEN). The sensitivity, analytical sensitivity, LOD and LOQ for effluent samples are presented in Table 5. Since different expressions have been used to calculate the figures of merit between different algorithms, these values cannot be directly compared with each other. But it can be stated that in most of the cases, where there was a sever coelution problem (e.g. regions 2 and 3 of the effluent sample), there was an increment in LOD and LOQ values, while comparing second-order with zero-order data. On the other hand, an enhancement in sensitivity (showed by improved LOD value) observed in case of AMOX and OFL, which could be related to the small contribution of interfering constituents and also exploiting multiple measurements and noise averaging. For SMX, a

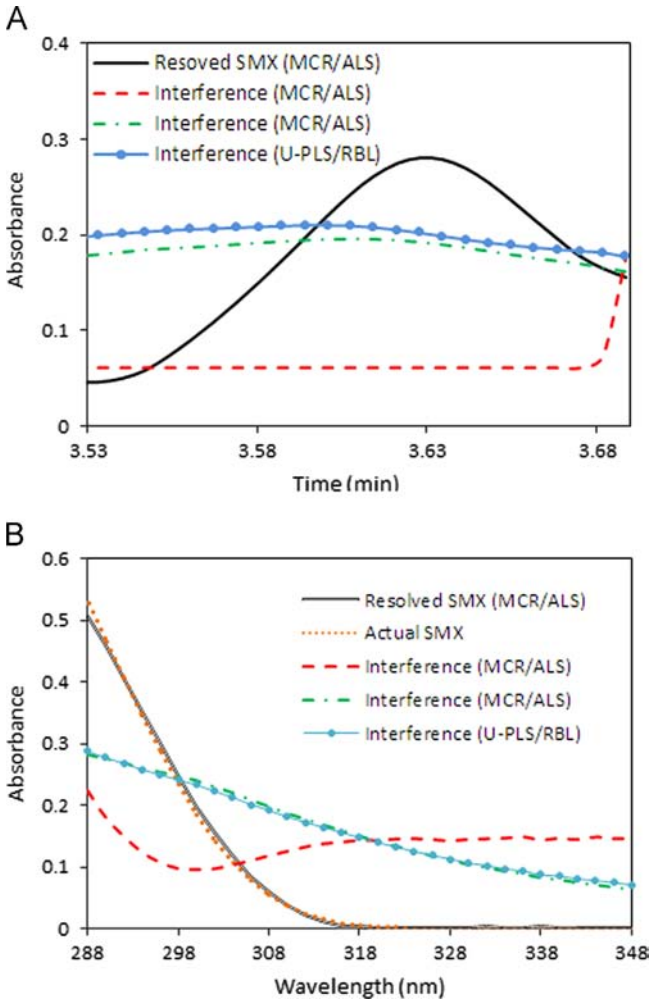

Fig. 5. Elution time profile of SMX (*black solid line*) recovered by MCR/ALS of in the presence of two interferences together with the time profile of the unexpected component retrieved by U-PLS/RBL on sample SI-3(A). Spectral profiles of SMX and interferences in the same sample extracted by MCR/ALS together with the spectral profile of unexpected component extracted by U-PLS/RBL (B). Normalized pure target spectrum (*red dot line*) for SMX has been superimposed, too. (For interpretation of the references to color in this figure legend, the reader is referred to the web version of this article.)

decrement in LOD value can be observed for MCR/ALS compared with U-PLS/RBL and univariate calibration. However, by comparing different complexity problems encountered in the multivariate analysis of the five regions and regarding the sensitivity improvement using the multivariate data, the magnitude of the mentioned multivariate figures of merit can be considered as satisfactory.

3.2.2. *Influent samples*

The described rapid strategy was also applied for determination of the selected antibiotics in wastewater treatment influent, as a more complex sample, when compared with STP effluent. The higher complexity of the typical influent chromatogram can be appreciated from Fig. 2. All validation samples were analyzed separately and in separate sub-matrices with the corresponding 15 calibration samples. As stated before, the most important challenge in this work was handling the data matrices without preprocessing steps. So, for proper handling of data sets with non-trilinear structure in the time direction, MCR/ALS was assigned to be used first, by constructing column-wise augmented data matrices. All mentioned five regions were analyzed using MCR/ALS. Attempts to resolve the analytes were successful for all regions with the component number pointed out in Table 3, except for the first and the second regions.

Fig. 5(A) shows the recovered elution profiles from decomposition of augmented data matrix corresponding to region 5 for analyzing SMX in sample SI-3. The actual and predicted spectral profiles of the analyte in the influent wastewater sample, in the presence of two interfering components, are shown in Fig. 5(B). The high spectral matching between true and resolved SMX profiles is clear in this figure. In fact, validation of predicted results for all analytes in all validation samples was internally checked through inspecting the similarity of the recovered spectral profiles to the actual profiles, and also the unimodality and non-negativity of the chromatographic profiles.

Because of the strong spectral similarity with sample matrix, and also the complexity of the selected sub-matrix, the overall results of MCR/ALS for region2 was somehow discouraging. So, in the next step, this region was further divided into two regions (see Table 3) and each region was analyzed separately. Once MCR/ALS was applied on the newly developed regions 2 and 3of the influent samples, two and four components were detected and resolved, respectively. The good quality of the resolved chromatographic

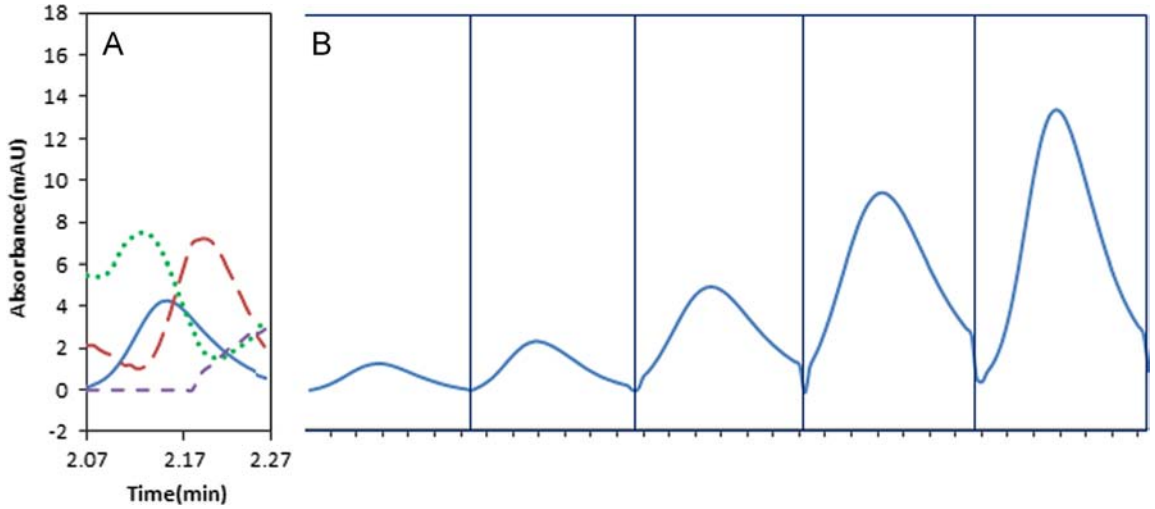

Fig. 6. Estimated elution time profiles corresponding to analysis of third region (containing MET) of influent wastewater sample data matrix (2.07–2.27 min). Four components (one analyte and three interferences) have been found by MCR–ALS analysis on sample SI-4(A). The solid blue line corresponds to MET profile, while the other profiles represent the recovered interfering profiles. The remaining five standard samples of MET profiles have been selected to show among the 15 calibration samples (B). (For interpretation of the references to color in this figure legend, the reader is referred to the web version of the article)

profiles for region 3 of sample SI-4 (as the most complex sub-matrix) together with the successive elution profiles for five calibration samples can be appreciated in Fig. 6. As can be seen, very strong coelutions between MET (blue solid line) and two matrix interferents (red long dash line and green dot line) were present. Very similar elution profiles at different investigated concentration levels were obtained for the analysis of MET in all other spiked samples and highly acceptable chromatographic and spectral profiles were obtained. The resolved profiles were also acceptable for the region 2 and modeling of SDZ. Once the MCR/ALS modeling with $N=4$was done, the quantitative analyses were performed for all validation samples by building a pseudo-univariate score-concentration calibration curve and interpolation of the analyte score into this plot.

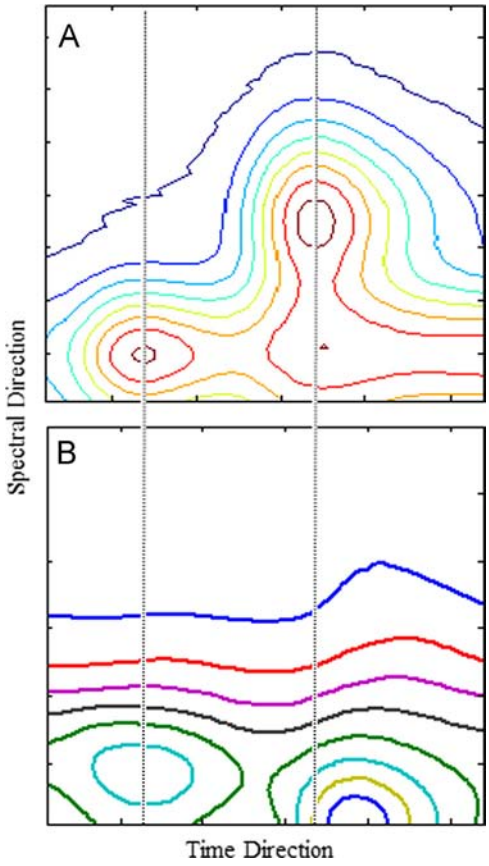

Fig. 7. Selected contour plots in the spectral-time region for SDZ and MET in a calibration sample (A) and a validation influent wastewater sample (B). The left and right dashed lines show the alignment of SZD and misalignment of MET, respectively.

The performance of U-PLS/RBL was also investigated through analysis of the aligned influent validation matrices. So, five predefined regions, as for the effluent samples, were considered first. But, in contrast to MCR/ALS, in which visual inspection of resolved analytes was a rather preliminary validation test, this was not the case for U-PLS/RBL. So, the predictive ability of the latter method was studied by means of the recovery values and statistical parameters. The comparison studies were performed for the data sub-sets which had been confirmed to have a single unexpected component. Therefore, considering the quantitative results with the proper number of unexpected components, the best results were obtained for regions 3–5. Quality of the resolved temporal and spectral profiles of one unexpected component in retention time region of SMX (last region), obtained using RBL, can be seen from Fig. 5(A) and (B), presented by the line marked with blue circles. As can be appreciated from this figure, there is a strong similarity between the mentioned unexpected component and the main interfering component extracted through MCR/ALS modeling (green dash dot line).

The poor recovery values for the second region can be attributed to the improper simultaneous chromatographic alignment of SDZ and MET, as can be seen in Fig. 7, which shows the contour plots for two different runs; the calibration sample (upper plot) and the validation sample. The proper alignment of SDZ in the presence of non-linear shift of MET is clear in this figure. So, after division of this region into two subsets, each region was separately aligned according to the Ref. [34] and modeled with U-PLS/RBL. The results showed that despite complexity of the region, acceptable recovery values could be obtained in each sub-region. Table 6 summarizes the predicted concentration values and also the parameters RMSEP and REP% obtained for the six antibiotics by the two algorithms, in the influent wastewater validation set (Table 1). Except

Table 6
MCR–ALS and U-PLS/RBL predicted concentrations on the validation samples obtained by spiking different antibiotics amount on a real influent wastewater sample.

Sample	Component ($\mu g\ L^{-1}$)[a]					
	AMOX	SDZ	MET	SMR	OFL	SMX
MCR–ALS						
Unspiked	92.9	27.7	−0.6	36.7	6.3	16.7
SI-1	10.6 (22)	10.7 (87.9)	6.7 (103.6)	4.1 (47.7)	9.7 (132.6)	7.3(100.5)
SI-2	n.d.[b]	6.0 (126.3)	6.9 (98.9)	3.4 (161.9)	8.9 (88.1)	5.4 (112.2)
SI-3	21.9 (71.6)	24.4 (75.1)	48.4 (110.0)	34.4 (78.9)	33.0 (108.2)	18.1(105.4)
SI-4	2.2 (12.1)	13.7 (92.6)	7.8 (94.6)	6.2 (140.9)	24.8 (102.4)	20.4 (139.0)
SI-5	17.1(42.2)	32.9 (72.8)	11.0 (77.0)	27.4 (75.8)	43.6 (106.1)	47.4 (116.1)
SD[b]	3.12	0.41	0.48	0.64	3.61	1.72
RMSEP ($\mu g\ L^{-1}$)	21.8	6.6	2.4	6.1	1.9	3.9
REP (%)	66.9	25.2	11.5	23.7	7.7	18.6
U-PLS/RBL						
Unspiked	74.8	24.5	−0.5	16.3	2.2	14.9
SI-1	15.3 (31.8)	13.9 (113.8)	5.4 (83.1)	11.5 (133.7)	5.9 (80.8)	4.0 (54.8)
SI-2	0.43 (4.2)	5.6 (117.9)	5.9 (84.3)	2.7 (128.5)	9.1 (90.1)	2.9 (60.0)
SI-3	20.6 (67.3)	34.2 (105.2)	50.3 (114.3)	36.7 (84.2)	25.7 (84.2)	12.2 (70.9)
SI-4	3.8 (20.8)	16.5 (111.5)	7.2 (86.7)	5.7 (129.5)	22.9 (94.6)	12.5 (85.6)
SI-5	16.4 (40.4)	33.4 (73.9)	14.9 (104.2)	27.8 (76.8)	35.6 (86.6)	33.9 (83.1)
SD[b]	4.52	1.61	0.23	0.66	0.72	1.51
RMSEP	20.3	5.4	2.9	5.0	3.4	4.2
REP (%)	62.2	20.6	13.7	19.7	13.1	20.1

[a] Values between parentheses correspond to recovery % of spiked amount.
[b] Standard deviation values for three replicates analysis of sample SI-5.

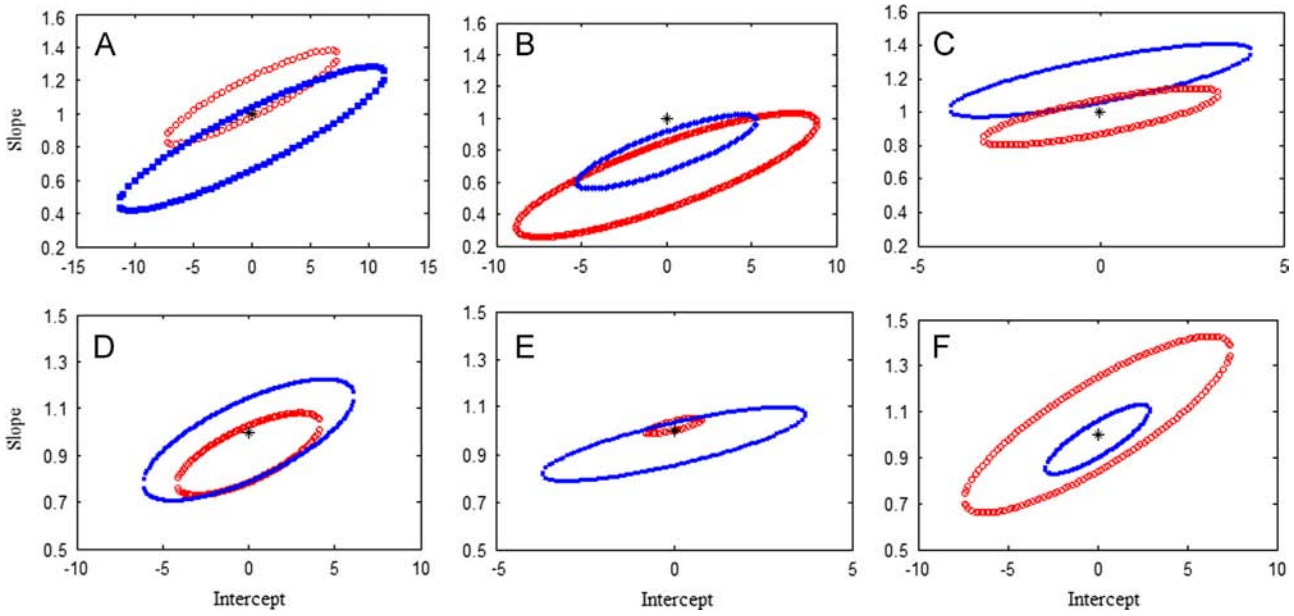

Fig. 8. Elliptical joint confidence region (EJCR) plot at 95% confidence limit, obtained through regression of found versus added concentration levels of antibiotics in whole validation samples (except for AMOX which only the effluent samples have been considered) using MCR/ALS (red circle markers) and U-PLS/RBL (blue square markers). (A) AMOX, (B) SDZ, (C) MET, (D) SMR, (E) OFL and (F) SMX. The black asterisk in the elliptical plots shows the theoretical (intercept=0, slope=1) point. (For interpretation of the references to color in this figure caption, the reader is referred to the web version of this article.)

for AMOX, the prediction values are acceptable in all of the cases, considering the high complexity of the sample matrices. On the other hand, the prediction results for AMOX through modeling by both algorithms were rather poor. However, in spite of discouraging quantitative analysis for AMOX, except for sample SI-2 which no chromatographic signal for AMOX was detected, qualitative results using MCR/ALS were still acceptable (results were not shown) in this region.

Moreover, in order to get further insight into the accuracy and precision of two mentioned algorithms, a linear regression analysis of nominal versus found concentration values in whole wastewater samples (except for AMOX in which just effluent samples have been considered) was implemented. The estimated intercept and slope were compared with their ideal values of 0 and 1using the elliptical joint confidence region (EJCR) test, at the probability level of 95% [56]. EJCR plots, resulted from MCR/ALS and U-PLS/RBL algorithms, have been depicted in Fig. 8(A)–(F), corresponding to the six analytes. As can be seen, except for SDZ and MET, all ellipses contain the theoretically expected points of (0, 1) for the intercept and slope and further proved the accuracy of the estimated concentrations. Also, for AMOX, MET, SMR and OFL, the elliptic size obtained with MCR/ALS is smaller, suggesting that this methodology shows higher precision for determination of these analytes when compared with U-PLS/RBL. On the other hand, the ellipses obtained through both modeling methods for SDZ do not jointly contain the ideal point (0, 1) (although, very close to that), which is indicative of the presence of a small proportional error. Fig. 8(C) shows the better predictive ability of MCR/ALS for MET determination. Finally, considering the whole predicted concentration values for all analytes in two wastewater samples with completely different interfering patterns, comparable predictive ability with relative advantage of MCR/ALS can be reported.

4. Conclusion

In this study, the performance of two second-order calibration algorithms MCR/ALS and U-PLS/RBL has shown and compared through a fast, easy and efficient direct injection HPLC–DAD strategy for determination of six antibiotic compounds in wastewater samples with different complexity. Both algorithms yielded good results in most of the cases where significant signal overlapping was detected. Also, comparable results were obtained with two algorithms for modeling the augmented data matrices in the presence of the least intensive and the most intensive interfering components in the studied wastewater samples. On the other hand, spectral similarities between the components had more adverse effects on the qualitative and quantitative results of MCR/ALS modeling compared with U-PLS/RBL. On the contrary, MCR/ALS was a more flexible algorithm than U-PLS/RBL for modeling data sets with a non-trilinear structure.

The use of short column has several significant benefits for multi-target analysis in high throughput screenings. However, in case of the need to attain lower LOD values, a pre-concentration step (as off-line or on-line) can be performed, considering the sample complexity. The proposed strategy showed that the combination of the mentioned algorithms to resolve the overlapping chromatographic signals allowed significant reducing in the run time and the complexity of the analysis. So, analyses were carried out with minimum chromatographic optimization efforts and using small amounts of organic solvents. However, some requirements should be met for proper resolution and quantification by MCR/ALS and U-PLS/RBL, such as suitable partitioning of the temporal-wavelength matrix for both algorithms, considering spectral similarity for modeling with MCR/ALS and proper chromatographic alignment before applying U-PLS/RBL.

Acknowledgments

The work was financially supported by the Iran National Science Foundation (Project no.92000051).

References

[1] M.C. Ortiz, L. Sarabia, J. Chromatogr. A 1158 (2007) 94–110.
[2] J.M. Amigo, T. Skov, R. Bro, Chem. Rev. 110 (2010) 4582–4605.

[3] M.M. Galera, M.D. García, H.C. Goicoechea, Trends Anal. Chem. 26 (2007) 1032–1041.
[4] M. Vosough, N.R. Mojdehi, Talanta 85 (2011) 2175–2181.
[5] M. Vosough, H.M. Esfahani, Talanta 113 (2013) 68–75.
[6] R.M. Maggio, P.C. Damiani, A.C. Olivieri, Talanta 83 (2011) 1173–1180.
[7] E. Peré-Trepat, S. Lacorte, R. Tauler, Anal. Chim. Acta 595 (2007) 228–237.
[8] M.M. Galera, M.D. Gil García, M.J. Culzoni, H.C. Goicoechea, J. Chromatogr. A1217 (2010) 2042–2049.
[9] M. Vosough, Sh. Ghafghazi, M. Sabetkasaei, Talanta 119 (2014) 17–23.
[10] J.A. Arancibia, P.C. Damiani, G.M. Escandar, G.A. Ibañez, A.C. Olivier, J. Chromatogr. B 910 (2012) 22–30.
[11] H.C. Goicoechea, M.J. Culzoni, M.D. Gil Garcia, M.M. Galera, Talanta 83 (2011) 1098–1107.
[12] M.J. Culzoni, R.Q. Aucelio, G.M. Escandar, Anal. Chim. Acta 740 (2012) 27–35.
[13] M. Vosough, M. Bayat, A. Salemi, Anal. Chim. Acta 663 (2010) 11–18.
[14] M. Vosough, A. Salemi, Food Chem. 127 (2011) 827–833.
[15] Y. Zhang, H.L. Wu, A.L. Xia, Q.J. Han, H. Cui, R.Q. Yu, Talanta 72 (2007) 926–931.
[16] X.D. Qing, H.L. Wu, Ch.Ch. Nie, Y. Li, X.F. Yan, X.H. Zhang, X.L. Yin, R.Q. Yu, Sci. Chin. Chem 56 (2013) 1641–1650.
[17] K.S. Booksh, B.R. Kowalski, Anal. Chem. 66 (1994) 782A–791A.
[18] E. Sanchez, B.R. Kowalski, Anal. Chem. 58 (1986) 496–499.
[19] E. Sánchez, B.R. Kowalski, J. Chemom. 1 (1990) 29–45.
[20] R. Bro, Chemom. Intell. Lab. Sys. 38 (1997) 149–171.
[21] H.A.L. Kiers, J.M.F. Ten Berge, R. Bro, J. Chemom. 13 (1999) 275–294.
[22] H.L. Wu, M. Shibukawa, K. Oguma, J. Chemom. 12 (1998) 1–26.
[23] Z.P. Chen, H.L. Wu, J.H. Jiang, Y. Li, R.Q. Yu, Chemmom. Intell. Lab. Syst. 52 (2000) 75–86.
[24] A.L. Xia, J.L. Wu, D.M. Fang, Y.J. Ping, L.Q. Hu, R.Q. Yu, J. Chemom. 19 (2005) 65–76.
[25] R. Tauler, Chemom. Intell. Lab. Syst. 30 (1995) 133–146.
[26] A. de Juan, R. Tauler, J. Chromatogr. A 1158 (2007) 184–195.
[27] M. Linder, R. Sundberg, Chemom. Intell. Lab. Syst. 42 (1998) 159–178.
[28] H.A.L. Kiers, J. Chemom. 14 (2000) 105–122.
[29] R. Bro, J. Chemom. 10 (1996) 47–61.
[30] J. Öhman, P. Geladi, S. Wold, J. Chemom. 4 (1990) 79–90.
[31] J. Öhman, P. Geladi, S. Wold, J. Chemom. 4 (1990) 135–146.
[32] A.C. Olivieri, J. Chemom. 19 (2005) 253–265.
[33] G.M. Escandar, H.C. Goicoechea, A.M. de la Peña, A.C. Olivieri, Anal. Chim. Acta 806 (2014) 8–26.
[34] B.J. Prazen, R.E. Synovec, B.R. Kowalski, Anal. Chem. 70 (1998) 218–225.
[35] K.J. Johnson, B.J. Prazen, D.C. Young, R.E. Synovec, J. Sep. Sci. 27 (2004) 410–416.
[36] E. Comas, R.A. Gimeno, J. Ferré, R.M. Marcé, F. Borrull, F.X. Rius, J. Chromatogr.A 1035 (2004) 195–202.
[37] S.A. Bortolato, J.A. Arancibia, G.M. Escandar, A.C. Olivieri, Chemom. Intell. Lab. Syst. 101 (2010) 30–37.
[38] F. Marini, A. D´Aloise, R. Bucci, F. Buiarelli, A.L. Magrí, A.D. Magrí, Chemom. Intell. Lab.Syst. 106 (2011) 142–149.
[39] J.M. Amigo, M.J. Popielarz, R.M. Callejón, M.L. Morales, A.M. Troncoso, M. A. Petersen, T.B Toldam-Andersen, J. Chromatogr. A 1217 (2010) 4422–4429.
[40] F. Cãnada-Cãnada, J.A. Arancibia, G.M. Escandar, G.A. Ibãnez, A.E. Mansilla, A. Mũnoz de la Peña, A.C. Olivieri, J. Chromatogr. A 1216 (2009) 4868–4876.
[41] M.D. Gil García, M.J. Culzoni, M.M. De Zan, R. Santiago Valverde, M.M. Galera, H.C. Goicoechea, J. Chromatogr. A 1179 (2008) 115–124.
[42] M.J. Culzoni, A.V. Schenone, N.E. Llamas, M. Garrido, M.S. Di Nezio, B.S. Fernández Band, H.C. Goicoechea, J. Chromatogr. A 1216 (2009) 7063–7070.
[43] M.R. Alcaráz, G.G. Siano, M.J. Culzoni, A.M. de la Peña, H.C. Goicoechea, Anal. Chim. Acta 809 (2014) 37–46.
[44] A.A.M. Stolker, W. Niesing, E.A. Hogendoorn, J.F.M. Versteegh, R. Fuchs, U.A. T. Brinkman, Anal. Bioanal. Chem. 374 (2004) 955–963.
[45] D. Perret, A. Gentili, S. Marchese, A. Greco, R. Curini, Chromatographia 63 (2006) 225–232.
[46] A.L. Batt, S. Kim, D.S. Aga, Chemosphere 68 (2007) 428–435.
[47] K. Kümmerer, Clin. Microbiol. Infect. 9 (2003) 1203–1214.
[48] F. Hernández, J.V. Sancho, M. Ibáñez, C. Guerrero, Trends Anal. Chem. 26 (2007) 466–485.
[49] S. Teixeira, C. Delerue-Matos, A. Alves, L. Santos, J. Sep. Sci. 31 (2008) 2924–2931.
[50] K. Yu, B. Li, T. Zhang, Anal. Chim. Acta 738 (2012) 59–68.
[51] W. Windig, J. Guilment, Anal. Chem. 63 (1991) 1425–1432.
[52] A.C. Olivieri, H.L. Wu, R.Q. Yu, Chemom. Intell. Lab. Syst 96 (2009) 246–251.
[53] EURACHEM guidance document no. 1 WELAC guidance document no. WGD 2 “accreditation for chemical laboratories: guidance on the interpretation of the EN 45000 series of Standard and ISO/IEC Guide 25”, available from the EURACHEM Secretariat, Teddington, Middle-sex, UK, 1993.
[54] M.C. Bauza, G.A. Ibañez, R. Tauler, A.C. Olivieri, Anal. Chem. 84 (2012) 8697–8706.
[55] F.A. Allegrini, A.C. Olivieri, Anal. Chem. 84 (2012) 10823–10830.
[56] A.G. González, M.A. Herrador, A.G. Asuero, A.G. González, Talanta 48 (1999) 729–736.